

Event-Related fMRI: Characterizing Differential Responses

K. J. Friston,* P. Fletcher,* O. Josephs,* A. Holmes,* M. D. Rugg,*† and R. Turner*

*The Wellcome Department of Cognitive Neurology, Institute of Neurology, Queen Square, London WC1N 3BG, United Kingdom; and †Wellcome Brain Research Group, School of Psychology, University of St Andrews, St Andrews, Fife KY16 9JU, United Kingdom

Received April 17, 1997

We present an approach to characterizing the differences among event-related hemodynamic responses in functional magnetic resonance imaging that are evoked by different sorts of stimuli. This approach is predicated on a linear convolution model and standard inferential statistics as employed by statistical parametric mapping. In particular we model evoked responses, and their differences, in terms of basis functions of the peri-stimulus time. This facilitates a characterization of the temporal response profiles that has a high effective temporal resolution relative to the repetition time. To demonstrate the technique we examined differential responses to visually presented words that had been seen prior to scanning or that were novel. The form of these differences involved both the magnitude and the latency of the response components. In this paper we focus on bilateral ventrolateral prefrontal responses that show deactivations for previously seen words and activations for novel words. © 1998 Academic Press

Key Words: event related response; functional neuroimaging; fMRI; hemodynamic response function; memory.

INTRODUCTION

We have recently described how to detect the hemodynamic responses evoked by single events in functional magnetic resonance imaging (fMRI) using linear (Josephs *et al.*, 1997) and nonlinear (Friston *et al.*, 1997) models. In this paper we consider how to detect, and make inferences about, the differences among event-related responses elicited by different sorts of events. We will also comment upon how to characterize the nature of these differences, with particular reference to the differential latency of evoked responses in a given region.

fMRI has the capacity to measure hemodynamic responses to changing stimulus or task conditions with a high spatial and temporal resolution. Its sensitivity is sufficient to detect the transient changes in deoxyhemoglobin concentration that follow the presentation of single stimuli (Boynton *et al.*, 1996; Buckner *et al.*,

1996). The techniques we have used (Josephs *et al.*, 1997; Friston *et al.*, 1997) to identify these changes model responses in terms of basis functions of peri-stimulus time, using the general linear model for statistical inference (in this case a multiple regression analysis). This sensitivity engenders a distinction between *event-related fMRI* and *state-related fMRI* where, in the latter, hemodynamic responses to changes in brain state are measured by asking subjects to engage in a sensorimotor or cognitive task for extended periods of time (i.e., epochs of a particular condition). The importance of event-related fMRI is that it allows the response to a single event to be examined in a context-independent fashion. State-related fMRI implicitly measures stimulus-induced responses in the context of repeated stimuli or continuous performance that itself may influence responses to the individual constituent events (e.g., by engaging a particular attentional set or introducing time-dependent changes in the nature of the response, such as habituation). Clearly the next step in event-related fMRI is to characterize the differences in evoked responses elicited by: (i) different classes of stimuli or (ii) the same stimuli in different response or attentional contexts. The importance of being able to characterize differential event-related responses is clearly exemplified in electrophysiology where many of the more interesting phenomena are revealed by comparing the evoked response to one stimulus type to that of another: for example, the “old/new” effect in recognition memory (Rugg, 1995). This example is particularly apposite given the nature of the exemplar fMRI experiment presented below.

This paper is divided into two sections. In the first we will review the background to modeling, and making statistical inferences about, event-related responses and describe the extension to this approach that is required to make inferences about the differences in these evoked responses. We will introduce the $SPM\{F\}$ (a statistical parametric map of the F statistic) as a device to detect responses throughout the brain and then comment on how one might characterize these differences in more detail. The second section applies the theory of the first section to a multisubject fMRI

study of visually presented words. The stimuli employed were either novel (in the context of the experiment) or had been subject to encoding just prior to scanning. We will use these exemplar data to demonstrate differential responses expressed in terms of the magnitude of the response and in terms of the response latency, in relation to stimulus onset. This paper is concerned with the theoretical aspects of the analysis. A neurobiological interpretation of these data will be presented separately.

THEORETICAL BACKGROUND

The Statistical Model of Evoked Responses

In Friston *et al.* (1994) we presented a model of observed hemodynamic responses, in fMRI time-series, that obtains when the underlying neuronal activity (inferred on the basis of changing task conditions) is convolved, or smoothed with a *hemodynamic response function*. This model was subsequently elaborated in the context of the general linear model (Friston *et al.*, 1995a, b; Worsley and Friston, 1995) and has been employed recently in the analysis of event-related responses (Josephs *et al.*, 1997; Friston *et al.*, 1997). This model can be thought of as a first-order approximation to a Volterra series expansion with finite “memory” T , relating the observed hemodynamic time series $y(t)$ at a given voxel to a set of stimulus functions $u_i(t)$ representing the repeated occurrence of the i th stimulus type:

$$y(t) \approx \eta^0 + \sum_i \int_0^T \eta_i(\tau) \cdot u_i(t - \tau) d\tau. \quad (1)$$

In this formulation the coefficients or kernel $\eta_i(\tau)$ corresponds to the hemodynamic response function for the i th stimulus. The next step, in making the estimation of η^0 and $\eta_i(\tau)$ more tractable, is to expand the kernels in terms of a small number of temporal basis functions $b_j(\tau)$:

Let

$$\begin{aligned} \eta^0 &= \gamma^0, \\ \eta_i(\tau) &= \sum_j \gamma_{ij} b_j(\tau). \end{aligned} \quad (2)$$

The basis functions can be chosen to provide a comprehensive but parsimonious model for the evoked responses. We generally use Fourier basis functions or mixtures of gamma functions and their derivatives. The advantage of Fourier functions is that they are insensitive to artifactual differences in the timing of the stimuli and the acquisition of data (as might be seen in sequential multislice acquisition). The advantage of non-Fourier basis functions is that they can be de-

signed to span the space of likely responses in a much more compact way. In this paper we use a very simple basis set: a synthetic hemodynamic response function and its derivative (see Fig. 1). The hemodynamic response function comprised the sum of two gamma functions and models a hemodynamic response with a slight undershoot typical of our data. Gamma functions provide reasonable and comprehensive models of the hemodynamic response function (Friston *et al.*, 1994; Boynton *et al.*, 1996). The inclusion of derivatives allows for differential latencies, in the response, among different brain areas and some latitude when (mis)specifying the onset of the stimulus relative to when the data were actually acquired.

We now create a new set of explanatory variables $v_{ij}(t)$ which represent the original stimulus functions $u_i(t)$ convolved with the j th basis function

$$v_{ij}(t) = \int b_j(\tau) \cdot u_i(t - \tau) d\tau;$$

substituting these expression into Eq. (1) gives

$$y(t) \approx \gamma^0 + \sum_i \sum_j \gamma_{ij} v_{ij}(t)$$

or in matrix notation, including confounds and explicit error term:

$$\mathbf{y} = [\mathbf{X}_1 \mathbf{X}_2 \dots \mathbf{1} \mathbf{G}] \cdot \boldsymbol{\gamma} + \epsilon. \quad (3)$$

This is a general linear model with response variable \mathbf{y} , a column vector representing the observed time-series,

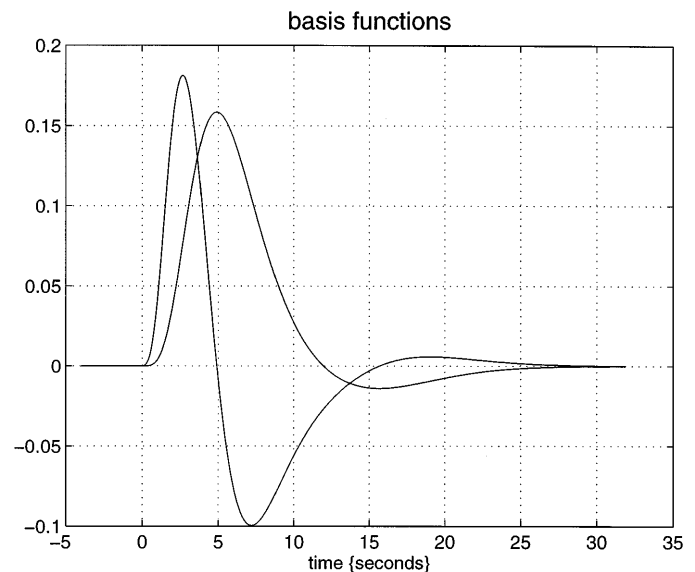


FIG. 1. Basis functions $b_j(\tau)$ used in the expansion of the response functions. These functions are a synthetic hemodynamic response function composed of two gamma functions (solid line) and its derivative (broken line). Both have been scaled to the same sum of squares.

a column vector of error terms ϵ , and a design matrix $\mathbf{X} = [\mathbf{X}_1 \ \mathbf{X}_2 \ \dots \ \mathbf{1} \ \mathbf{G}]$. $\mathbf{1}$ corresponds to a column of ones and \mathbf{G} is a collection of other uninteresting effects or confounds such as low-frequency artifacts. The partitions of the design matrix \mathbf{X}_i contain the explanatory variables $v_{ij}(t)$ for the i th event type, i.e., the convolved stimulus functions sampled at the times that the scans were acquired. The unknown parameters γ_{ij} and γ^0 constitute the initial elements of the column vector γ .

Making Inferences about Evoked Responses

Having formulated the model in this way we can now use standard procedures developed for serially correlated fMRI time-series that employ the general linear model (Friston *et al.*, 1995a; Worsley and Friston, 1995). These procedures provide parameter estimates (e.g., estimates of the basis function coefficients and, implicitly, the responses themselves) and statistical parametric maps (SPMs) testing the significance of all or some of the modeled response components. The parameter estimates \mathbf{g} of γ are computed using standard least-squares and are used to calculate the estimates $h_i(\tau)$ of the responses $\eta_i(\tau)$.

In the present context we are interested in making statistical inferences about (i) responses to any stimulus type and (ii) differential responses. To test for any response we can create an SPM $[F]$ testing for all the effects in $[\mathbf{X}_1 \ \mathbf{X}_2 \ \dots]$, treating the constant and other specified terms as confounds. P values, corrected for the volume analyzed, are then assigned to maxima in the ensuing SPM $[F]$ using the theory of Gaussian fields (Worsley, 1994).

The final step is to assess differential responses. In general this involves rearranging the design matrix so that we can distinguish between the evoked hemodynamic response common to all types of stimulus and the differences among these responses. The common responses are then treated as confounds and a new SPM $[F]$ is computed that tests for, and only for, the differences. The common or main effect is simply $\mathbf{X}_c = [\mathbf{X}_1 + \mathbf{X}_2 + \dots]$, the sum of all the stimulus-type-specific effects. The differences \mathbf{X}_d are given by orthogonalizing \mathbf{X} with respect to $\mathbf{X}_c = \mathbf{X} - \mathbf{X}_c \cdot \text{pinv}(\mathbf{X}_c) \cdot \mathbf{X}$. In the case of just two stimulus types, $\mathbf{X}_d = \mathbf{X}_1 - \mathbf{X}_2$. This “partitioning” of the design matrix into commonalities and differences leads to an equivalent linear model

$$\mathbf{y} = [\mathbf{X}_d \ \mathbf{X}_c \ \mathbf{1} \ \mathbf{G}] \cdot \gamma + \epsilon \quad (4)$$

and the SPM $[F]$ tests for the effects in \mathbf{X}_d , treating the remaining partitions as confounds. In the present example we can use a simpler approach and assess the differences directly using the original model [Eq. (3)] and a linear compound or contrasts of the parameter estimates to give a SPM $[t]$. This is because we have used a small and largely orthogonal basis set, where

the response itself can be associated with the synthetic hemodynamic response function and the effects modeled by the derivative can be interpreted as a shift of this response in time. To find increases in the response magnitude elicited by event type A, relative to B, we would specify a contrast that was 1 for A’s response function, -1 for B’s, and zero elsewhere. The square of the resulting SPM $[t]$ would be exactly the same as the equivalent SPM $[F]$, using Eq. (4), if the derivatives (i.e., timing effects) had been treated as confounds. We can test for differential latencies using a contrast of the derivatives in a similar way.

Estimating the Standard Error of Evoked Responses

A useful feature of using basis functions, when formulating the model as above, is that the estimated responses are continuous functions of time. This means we can estimate responses at latencies not actually measured. The estimated response to a particular stimulus, at time τ , is simply a linear compound of the parameter estimates weighted by the values of the basis functions at τ [from Eq. (2) $h_i(\tau) = \sum g_{ij} \cdot b_j(\tau)$]. This means that we can use standard results to obtain the standard error of the estimated response at τ , again as a continuous function of time $\text{SE}[h_i(\tau)]$. The Appendix (A.1) describes how to do this. An alternative characterization, of the reliability of the estimated response, would be to use confidence intervals. The confidence intervals follow simply from the standard error and their derivation is presented in the Appendix (A.2). In this paper we use the standard error.

Finally we can estimate the standard error of the timing of the response if we assume that the error in $h_i(\tau)$ is attributable to a stochastic error in timing τ^* , where each estimate of $h_i(\tau)$ is a realization of $\eta_i(\tau + \tau^*)$. The Taylor expansion

$$h_i(\tau) = \eta_i(\tau + \tau^*) = \eta_i(\tau) + \tau^* \cdot dh_i(\tau)/d\tau + \dots$$

allows one to posit

$$\text{SE}[h_i(\tau)] \approx \text{SE}(\tau^*) \cdot dh_i(\tau)/d\tau. \quad (5)$$

The standard error of these temporal perturbations is equivalent to the standard error of any estimated latency I_i (i.e., $\text{SE}[I_i] = \text{SE}(\tau^*)$), giving

$$\text{SE}[I_i] \approx \text{SE}[h_i(\tau)] / (dh_i(\tau)/d\tau). \quad (6)$$

We will use this result in the next section to estimate the temporal precision of event-related fMRI and to make inferences about differences in response latencies.

AN ILLUSTRATIVE APPLICATION

Experimental Design and Data Acquisition

In this section we apply the theory presented above to a fMRI time-series obtained from three normal subjects during exposure to visually presented words that were either (i) novel to the experiment or (ii) had been studied in an encoding task prior to scanning. The data were acquired at 2 T using a Magnetom VISION (Siemens, Erlangen) whole-body MRI system, equipped with a head volume coil. Contiguous multislice T_2^* -weighted fMRI images were obtained with a gradient echo-planar sequence using an axial slice orientation (TE = 40 ms, TR = 3.22 s, $64 \times 64 \times 16$ matrix size, $3 \times 3 \times 3$ mm voxels). After discarding the first few scans (to allow for magnetic saturation effects) the time-series comprised 480 volume images, per subject, with 3-mm isotropic voxels. Words were presented every 16 s in a pseudorandom order. The subject was asked to discriminate novel from studied words by a keypress using the middle or index finger of the right hand.

Data Preprocessing

The data were analyzed with SPM97 (Wellcome Department of Cognitive Neurology, <http://www.fil.ion.ucl.ac.uk/spm>). The time-series were realigned, corrected for movement-related effects, and spatially normalized into the standard space of Talairach and Tournoux (1988) using the subject's coregistered structural T_1 -weighted MRI scan (Friston *et al.*, 1995c, 1996). The data were spatially smoothed with a 4-mm isotropic Gaussian kernel and temporally smoothed with a 4-s Gaussian kernel.

Event-Related Responses

The data were analyzed using the design matrix in Eq. (3) to assess the effect of either stimulus type and to provide the stimulus-specific response estimates $h_1(\tau)$ and $h_2(\tau)$. The analysis of differential responses employed the appropriate contrasts, testing for differences in response magnitude and differences in response latency. The first analysis gives a SPM[F] testing for the significance of an event-related response to one or both stimulus types. The second analysis generates SPM[t]s reflecting the significance of any differential responses. We modeled the response to stimuli separately for each subject. This means that the parameters that identify the associated response functions were estimated independently for each subject, allowing us to assess the reproducibility of the form of differential responses from subject to subject. The data were normalized by dividing by the whole brain mean and multiplying by 100. The resulting effects are then expressed as a percentage of whole brain mean.

The basis functions used in these analyses are shown in Fig. 1. The stimulus functions $u_1(t)$ and $u_2(t)$ were set to unity at the presentation of each stimulus type and zero elsewhere. The SPM[F] reflecting the significance of evoked responses modeled in \mathbf{X}_1 and \mathbf{X}_2 (or more formally, testing the null hypothesis that all $h_1(\tau)$ and $h_2(\tau)$ were jointly zero) is shown in Fig. 2 with the design matrix. The left-hand side of the design matrix comprises the explanatory variables \mathbf{X}_1 and \mathbf{X}_2 . The remaining columns contain the constant $\mathbf{1}$ used to estimate g^0 and other effects designated as confounds (low-frequency artifacts). The partitions were arranged to yield subject-specific estimates. The SPM[F] has been thresholded ($P < 0.05$ corrected for multiple comparisons) and shows widespread responses, notably in the striate, extrastriate, medial parietal, anterior cingulate, right dorsolateral prefrontal cortex, left lingual and parahippocampal gyri, left sensorimotor cortex (hand area), and left inferior postcentral gyrus (BA 40). It can be seen that the most intense responses were elicited in the sensorimotor area associated with the executive components of the subjects' finger movements. Other extremely significant responses were observed in bilateral basal posterior temporal cortices. An example of an estimated evoked response, to old words, is shown in Fig. 3 for a voxel in the left sensorimotor area, in terms of the adjusted data (dots) and the estimated or fitted responses (solid lines). The standard error was computed as described in the Appendix and the broken line represents plus and minus one standard error. There are several important things to note about this characterization: (i) The standard error seems smaller than one might have predicted on the basis of the scatter of the adjusted data, because the estimated response at any single point in time is based on data from *all* points in time. This is a feature of using basis functions, as opposed to simply taking the average in some limited time window. In other words by using a parsimonious model of expected responses, the responses can be estimated with a greater degree of precision than when using a less specified model. (ii) It may be noted that the standard error of the response is zero when the estimated response is itself zero. Although this may seem counterintuitive it is entirely sensible: Although the response may actually differ from zero between stimuli, these effects are modeled by other components of the design matrix (e.g., the low-frequency confounds). (iii) It appears as if the evoked response starts before the onset of the stimulus. There are two factors that relate to this: The first is that the data (and the design matrix) were temporally smoothed in accord with the matched filter theorem (Friston *et al.*, 1995a). This convolution smears the initial responses into the prestimulus period. Second, the onset of the stimulus was defined in terms of the start of volume acquisition. In our mul-

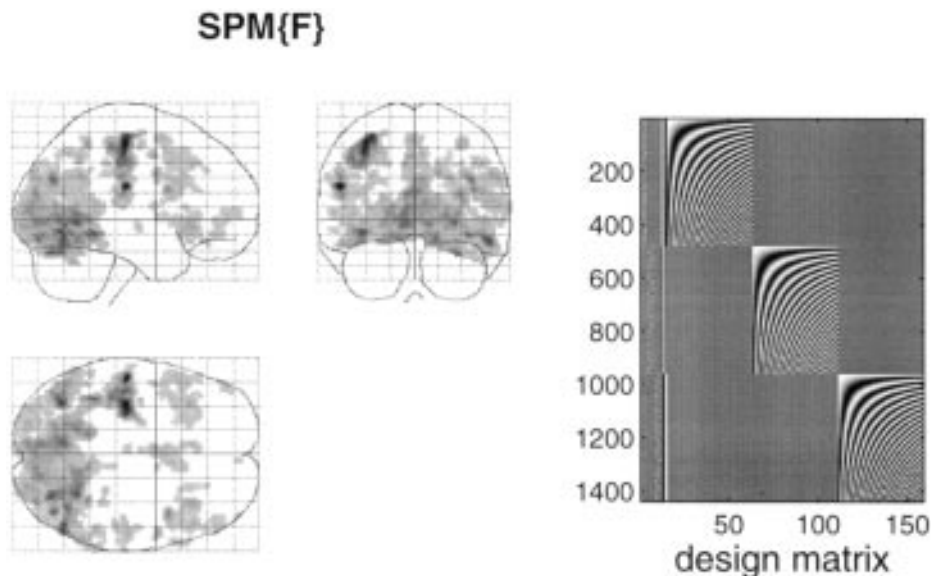


FIG. 2. (Left) $SPM\{F\}$ testing for the significance of event-related responses to either word type. This is a maximum intensity projection of a statistical image of the F ratio, following a multiple regression analysis at each voxel. The format is standard and provides three orthogonal projections in the standard space of Talairach and Tournoux (1988). The grayscale is arbitrary and the $SPM\{F\}$ has been thresholded at $P < 0.05$ (corrected). (Right) The design matrix used in this analysis. The design matrix comprises the explanatory variables in the general linear model. It has one row for each of the 3×480 scans and one column for each explanatory variable or effect modeled. The left-hand columns contain the explanatory variables of interest $v_{ij}(t)$ for each subject, where $v_{ij}(t)$ is word stimulus function $u_i(t)$ convolved with the basis function $b_j(\tau)$ in Fig. 1. The remaining columns contain covariates or effects of no interest designated as confounds. These include (left to right) a constant term and periodic (discrete cosine set) functions of time to remove low-frequency artifacts with a high-pass cutoff period of 64 s.

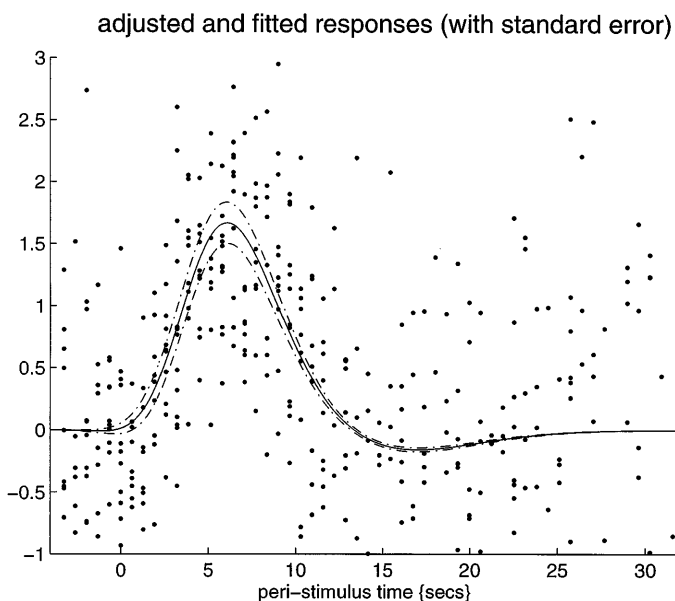


FIG. 3. Fitted response in the left sensorimotor area to previously seen words. This voxel represents the maximum of the $SPM\{F\}$ of the previous figure. The fitted response (solid line) is shown with the adjusted data (dots) plus and minus one standard error of the fitted response (broken lines). The adjusted data are the original data with confounds (and the response to previously seen words) removed. The data are plotted as a function of peri-stimulus time.

tislice acquisition it may be some time later that the data were actually acquired, meaning that the onset time, from the perspective of any voxel, could be earlier than 0 s. It would be possible to correct for this by shifting the data in time, as a preprocessing step, but in our sequential acquisition the use of temporal derivatives in the design matrix seems to be sufficient.

In most brain areas the responses evoked by novel and studied words were indistinguishable. An example is provided in Fig. 4 where the responses of the left parahippocampal gyrus ($-16, -44, -4$ mm) to the two sorts of stimuli are shown. These responses were highly significant ($F = 7.86, P < 0.001$ corrected). Figure 4 shows the estimated responses (solid lines) and standard errors (broken lines). It can be seen that the differences between the estimated responses are small compared to their respective standard errors and that there is little evidence for a differential response in this region.

Differential Responses

The subsequent analyses identified significant differences in several regions including the visual, inferotemporal, and prefrontal cortices. We will concentrate here on two examples that demonstrate the various forms that these differences can take. In the first we focus on a result that replicated not only over all three subjects

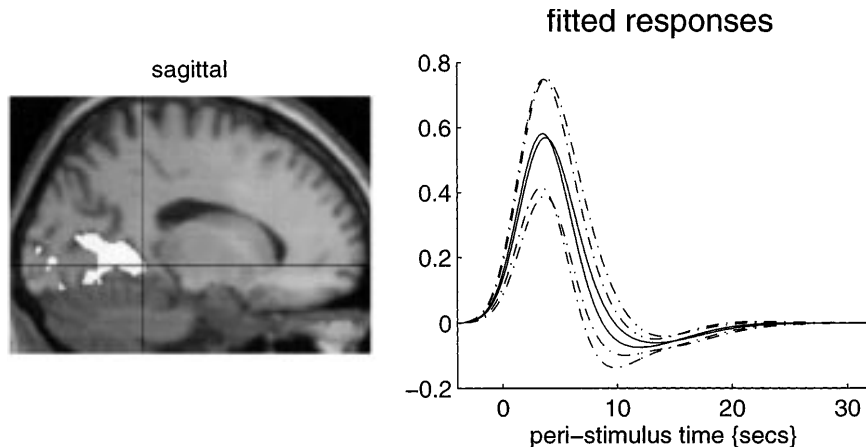


FIG. 4. (Left) $SPM[F]$ thresholded at $P < 0.05$ (corrected) superimposed on a structural MRI testing for a significant response to either word type. The posterior regions highlighted correspond to the lingual and parahippocampal gyri. (Right) Event-related responses at the voxel marked by the cross-hairs on the $SPM[F]$; $(-16, -44, -4 \text{ mm})$. The evoked responses are plotted in terms of estimated responses (solid lines) and their standard errors (broken lines) as a function of time following stimulus onset.

but was expressed bilaterally in homologous ventrolateral prefrontal regions. In these regions, again in all subjects, novel words elicited strong activations whereas words that had been seen previously evoked negative responses or deactivations (although in the third subject the response to old words was more biphasic). The results for each of the three subjects are shown separately in Figs. 5, 6, and 7. In each figure the responses are shown in terms of the fitted response (solid line) and standard error (broken lines). The inset corresponds to the $SPM[t]$ (after transformation to a $SPM[Z]$) showing all voxels above a threshold of $P = 0.05$ (uncorrected) on a standard structural MRI (coronal section). The cross-hairs locate the voxel whose response is depicted in the graph. For example in Fig. 5 this voxel come from the inferior frontal gyrus (BA 37). This differential effect is reasonably significant $Z = 4.18$ ($P < 0.001$ uncorrected). The Z scores for the voxels in the remaining subjects were 3.10 ($P = 0.001$ uncorrected, Fig. 6) and $Z = 3.59$ ($P < 0.001$ uncorrected, Figure 7).

Contrast the sort of differences in the previous section with those identified when testing for differential latencies. Figure 8 shows the responses of a voxel in the fusiform gyrus $(-38, -78, -10 \text{ mm}, Z = 4.14, P < 0.001$ uncorrected). As above, this differential effect was bilaterally represented and shows that novel words evoked a much earlier response than previously seen words. In this example response latencies were assessed by the time to reach a third of the response maximum. The differential latency (about 3 s) is relatively large compared with the standard errors of the timing of the responses. The black bars in Fig. 8 show these standard errors according to Eq. (6). The standard error for previously seen words was only 299 ms. This can be taken as the effective temporal resolution of

the response to this stimulus, in this area, and compares very favorably to the repeat time of 3.22 s. It is possible to make explicit inferences about differential onset latency using the standard errors of the timing as described in the Appendix (A.3). The examples given above demonstrate that the approach presented here is sensitive to differences in timing as well as to differences in the magnitude of response components. It should be noted that the differential response latencies observed are far in excess of those that might be predicted by electrophysiological studies.

DISCUSSION

We have presented an approach to characterizing the difference between hemodynamic responses in fMRI that are elicited by different sorts of stimuli. This approach is based on a linear convolution model and standard inferential statistics. In particular we have modeled evoked responses and their differences in terms of basis functions of peri-stimulus time. This facilitates a characterization of the response profiles that has a relatively high effective temporal resolution. We were able to demonstrate differences in both the magnitude and in the latency of hemodynamic responses to visually presented words, depending on whether or not the words had been processed prior to scanning. As a general point it is worth emphasizing that “response” in this paper refers to a stereotyped hemodynamic transient that is expressed relative to the prestimulus baseline. Thus, as with event-related potentials, the response is hard to interpret without reference to what the brain was doing during the baseline.

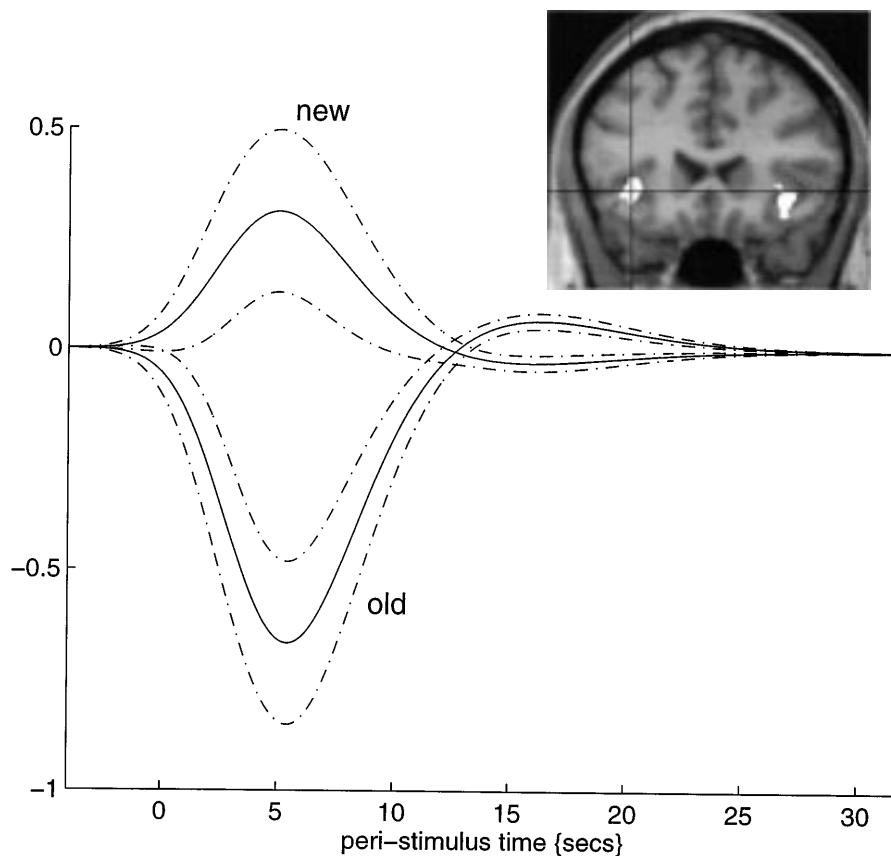


FIG. 5. (Inset) SPM $|Z|$ thresholded at $P < 0.05$ (uncorrected) superimposed on a structural MRI testing for a significant differential response in the first subject. The highlighted areas correspond to the inferior frontal sulci. (Graph) Event-related responses at the voxel marked by the cross-hairs in the inset; $(-38, 22, -4 \text{ mm})$. The evoked responses are plotted in terms of estimated responses (solid lines) and their standard error (broken lines) as a function of time following stimulus onset. Old denotes responses to previously seen words, and new denotes responses to novels words.

The Basis Functions

A key aspect of the approach presented here is the use of basis functions of peri-stimulus time. There are clear advantages to using basis functions, compared to simply averaging trial-based responses. Not least among these is the facility to increase effective temporal resolution well above the repetition time and indeed estimate responses as a function of continuous time. A more fundamental advantage is that it does not require the scans to be acquired with any fixed temporal relationship to the stimuli (this is because there is no *post hoc* binning of the data for averaging). This may be important in instances where the stimuli are not under experimental control (e.g., perceptual reversal during presentation of ambiguous figures). It is worthwhile considering that, using basis functions, the maximum effective temporal resolution is the interstimulus interval divided by the total number of scans, although in this instance there will be only one observation per peri-stimulus time point. The key point though is that the effective resolution is generally related to the

number of scans, not the repetition time. This is an important consideration when choosing the basis functions because it is possible to properly model temporal frequencies that are higher than would normally be allowed, given the limitations on temporal sampling imposed by the repetition time. Of course if one has restricted sampling to a small number of discrete points in peri-stimulus time, then the basis set should be chosen to reflect that fact.

The choice of basis functions is clearly a function of the nature of the data acquired and the questions being asked of them. In general we have found that more robust results obtain when the basis set is small and temporally compact, especially when the interstimulus interval is short. In this paper we have used perhaps the simplest set possible: a synthetic hemodynamic response function and its derivative. This precludes response forms that are substantially more protracted than the normal response to a short-lived burst of neuronal activity but was sufficient to give meaningful results in the present study. There are other situations

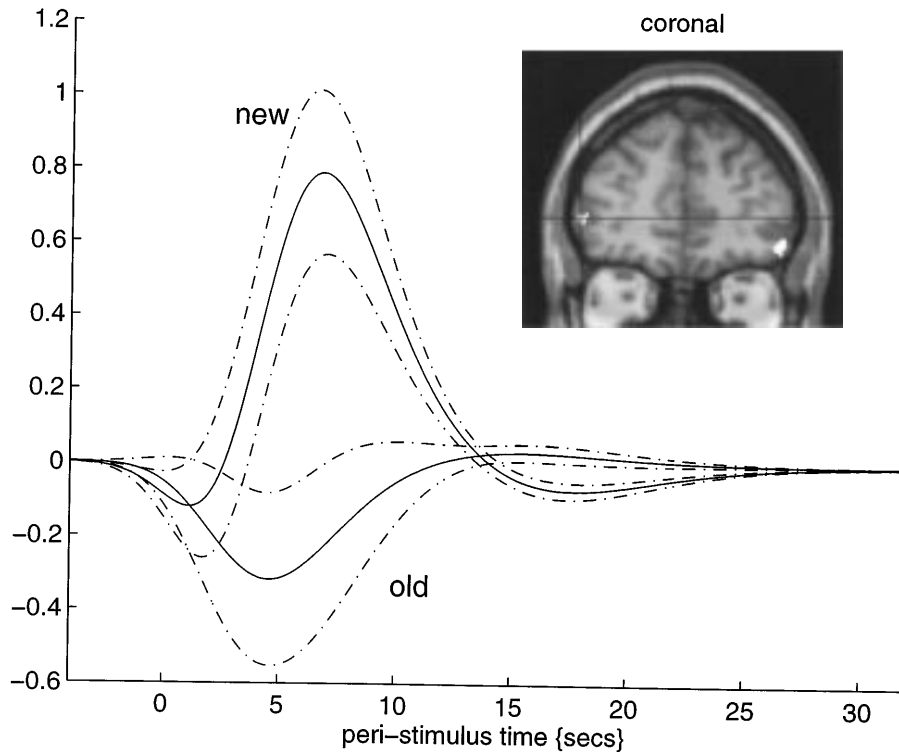


FIG. 6. As for Fig. 5 but showing differential responses in the second subject.

(e.g., sentence processing) when the neuronal time constants may call for more comprehensive sets of basis functions that span longer periods of time (e.g., Vandenberghe *et al.*, 1997). In the context of characterizing phasic events we are currently exploring the general approach of using the partial derivatives of a “canonical” response function. In this framework an arbitrary hemodynamic response function f is selected with a small number of model parameters p_i $f(t, p_1, p_2, \dots)$. The basis set would then comprise f , $\partial f / \partial t$, $\partial f / \partial p_1$, $\partial f / \partial p_2, \dots$. The simplest version of this has been used in this paper (i.e., f and $\partial f / \partial t$). The advantage of this approach is that each modeled effect in the design matrix has some physical meaning. Consequently contrasts of the associated parameter estimates can be interpreted. We have used this above to characterize differential responses in terms of differences in magnitude (testing for differences among the f) and differences in latency (differences among the $\partial f / \partial t$). We do, however, appreciate that differential responses may be very complicated and do not necessarily conform to this simple dichotomous classification.

A final point, in relation to the basis set employed, is one of collinearity or correlations among the basis functions. Generally this is not problematic from the point of view of statistical inference. Collinearity within a design matrix partition (e.g., interesting effects or confounds) has no effect on the ensuing statistical quotients when using the F statistic. The only problem

that can arise is when one looks at the parameter estimates in isolation (either in terms of estimated responses or inferences using the $SPM(t)$). In the present paper we avoided linear dependence among the basis functions by using a sufficiently long interstimulus interval and by using one function and its derivative for each stimulus type. In doing this we were able to use the $SPM(t)$ with impunity.

Response Latencies

One component of the work presented here is the characterization of differential responses in terms of response latency and the associated standard error. The standard errors of response onsets (as judged by the time to reach a third of the maximal response) suggest that in some instances fMRI can discriminate between dynamics on a 100-ms timescale despite relatively long repetition times. This is very encouraging but should not be confused with the notion that fMRI can be used to look at response latencies *among different areas* (as used in electrophysiology to infer the temporal sequence of areas that are recruited during the promulgation of neuronal dynamics from one area to the next). fMRI cannot be used to do this because of the endogenous regional variability in the latency of hemodynamic responses to underlying changes in neuronal activity (not to mention artifactual difference due to the timing of slice acquisitions) (DeYoe *et al.*, 1992).

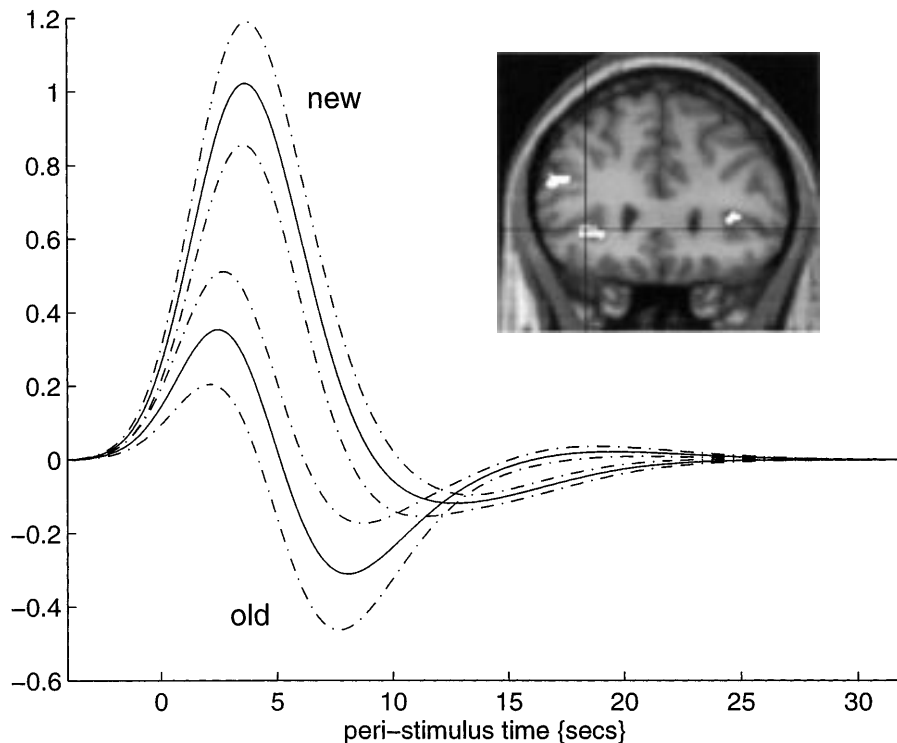


FIG. 7. As for Fig. 6 but showing differential responses in the third subject.

However, it is in principle possible, using the methods outlined above, to make inferences about the difference in differential response latencies between areas (i.e., stimulus 1 incurs a differential response latency of 650 ms, relative to stimulus 2, in area A but only 15 ms in area B). This would constitute a region \times stimulus-specific response latency interaction that would be independent of the (main) effect of region-specific differences.

We have elected to characterize latency differences in terms of the standard error of the onset time as opposed to the standard error of the response itself. This is in contradistinction to some techniques in electrophysiology where the differential latency is defined in terms of when the responses can be shown to be significantly different (e.g., Thorpe *et al.*, 1996). The fundamental distinction here is between defining an “onset time” based on the parameter estimates of the response (our approach) and defining it in terms of the standard error of the parameter estimates (the alternative based on the demonstration of a significant difference). We have adopted our approach for the obvious reason that the estimate of onset time should be a function of the expected response, not the error of its measurement.

Statistical Considerations

One aspect of the techniques presented in this paper is the use of the $SPM[F]$ to make inferences about the significance of responses and their differences. This is

another instance of the usefulness of the $SPM[F]$. The importance of the $SPM[F]$, as opposed to $SPM[t]$ or t maps, is that it reflects the significance of a whole set of parameter estimates, in this instance the collection of coefficients that describe the hemodynamic responses $[h_i(\tau)]$ or their differences (not reported in this paper). We envisage that the $SPM[F]$ will find an increasing role in fMRI as the models of hemodynamic responses become more sophisticated and the number of parameters increases. Some device is required to make an inferences about these parameters *en masse*. The $SPM[F]$ is one such device.

It should be noted that the model employed to create the SPMs was a linear convolution model relating a set of stimulus functions to the hemodynamic response. We have demonstrated previously (Friston *et al.*, 1997) that there are significant nonlinear components in hemodynamic responses; however, these are expressed when stimuli are presented close together in time (such that the response to one stimulus is modulated by the response to a preceding stimulus). In the context of event-related fMRI, with reasonable interstimulus intervals, these nonlinear effects can be discounted and one would normally be quite comfortable with a linear model of the sort described here.

Neurobiological Interpretation

Throughout this paper we have referred to the input $u_i(t)$ as a stimulus function and $y(t)$ as the hemody-

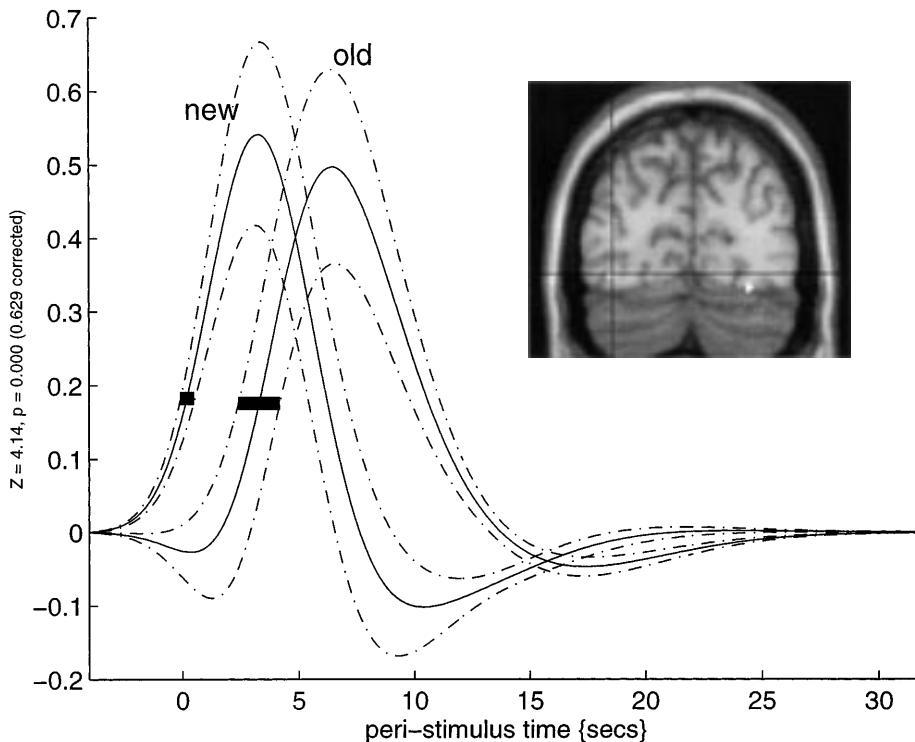


FIG. 8. As for the previous figures (Figs. 5–7) but in this instance showing an example where responses (of a single subject) differ in terms of their latencies. The evoked responses are plotted in terms of (i) estimated responses (solid lines), (ii) their standard error (broken lines), and (iii) the standard error of the time to third peak response (bars). This is for a voxel in the left fusiform gyrus ($-38, -78, -10$ mm).

dynamic response. One can conceptualize the components of the mapping from stimulus to response in terms of (i) a transformation of the stimulus into evoked neuronal dynamics and (ii) a translation of these neuronal changes into hemodynamic responses. If one demonstrates a significant difference among hemodynamic responses in the same area, then there are two explanations: (i) The stimuli elicited different patterns of neuronal activity or (ii) the hemodynamic response to neuronal transients has itself changed. Clearly we have assumed that the first is the proper explanation. However, it is possible that the relationship between neuronal dynamics and hemodynamic response may also have changed, for example, changes in cerebral physiology associated with hyperventilation during anxiety-provoking stimuli relative to neutral stimuli (here the resulting changes in global cerebral perfusion and relative oxygenation may be expressed in terms of a change in the hemodynamic responsiveness to underlying neuronal activation, i.e., a subtle change in the hemodynamic response function). On balance though, given that the stimuli are carefully chosen and well matched, in terms of both their attributes and the context in which they are presented, one might be quite justified in assuming that the hemodynamic response function in a given area will not change markedly. In such circumstances any difference in the hemodynamic

responses observed can be assigned to differential processing at a neuronal level.

Conclusion

We have presented a simple extension to previous models of evoked responses in event-related fMRI that allows for the characterization of differences among stimulus-specific responses using standard techniques developed for the analysis of functional neuroimaging data.

APPENDIX

A.1. The Standard Error of a Linear Compound of Parameter Estimates for Serially Correlated Data

In this section we derive the standard error for the estimated response $h_i(\tau)$ as a function of response latency τ . From Eq. (2) we have $h_i(\tau) = \sum g_{ij} \cdot b_j(\tau)$. Because we know both the standard error of the parameter estimates g_{ij} and the values of the basis functions at time τ , $b_j(\tau)$, we can derive the standard error of the estimated response at τ . In matrix notation $h_i(\tau) = \mathbf{b}_i(\tau) \cdot \mathbf{g}$ where, for example $\mathbf{b}_1(\tau) = [b_1(\tau), \dots, b_j(\tau), 0, \dots, 0]$ and similarly for \mathbf{b}_2 , \mathbf{b}_3 and so on. The standard error of the estimated responses is then given

by

$$\begin{aligned} \text{SE}[h_i(\tau)] &= \text{SE}[\mathbf{b}_i(\tau) \cdot \mathbf{g}] \\ &= \sigma \cdot \sqrt{(\mathbf{b}_i(\tau) (\mathbf{X}^* \mathbf{X}^*)^{-1} \mathbf{X}^{*T} \mathbf{V} \mathbf{X}^* (\mathbf{X}^* \mathbf{X}^*)^{-1} \mathbf{b}_i(\tau)^T)}, \end{aligned}$$

where

$$\begin{aligned} \mathbf{X}^* &= \mathbf{K} \mathbf{X} \\ \mathbf{V} &= \mathbf{K} \mathbf{K}^T \\ \sigma^2 &= \mathbf{y}^T \mathbf{R}^T \mathbf{R} \mathbf{y} / \text{tr}[\mathbf{R} \mathbf{V}], \end{aligned}$$

and where T denotes transpose and $\text{tr}[\cdot]$ the trace of a matrix. $\mathbf{y}^T \cdot \mathbf{R}^T \mathbf{R} \cdot \mathbf{y}$ is the sum of squares due to error. \mathbf{R} is the residual forming matrix ($\mathbf{I} - \text{pinv}(\mathbf{X})$), \mathbf{I} is the identity matrix, and \mathbf{V} is the autocovariance matrix that characterizes any serial correlations in the time-series (see Worsley and Friston, 1995, for details). If the data are independent then $\mathbf{V} = \mathbf{I}$.

A.2. Confidence Intervals for a Linear Compound of Parameters for Serially Correlated Data

In this section we derive the pointwise 95% confidence intervals (CI) for $\eta_i(\tau)$ using the standard error of its estimate from the previous section:

$$\text{CI} = h_i(\tau) \pm t_{\nu, 0.975} \cdot \text{SE}[h_i(\tau)],$$

where $t_{\nu, 0.975}$ is the 97.5 percentile of the t distribution with ν degrees of freedom and

$$\nu = \text{tr}[\mathbf{R} \mathbf{V}]^2 / \text{tr}[\mathbf{R} \mathbf{V} \mathbf{R} \mathbf{V}].$$

A.3. Testing the Null Hypothesis of a Differential Latency

Consider two response latencies I_1 and I_2 for two stimulus types at a particular voxel. If we assume that these estimated latencies are independent and normally distributed, then we can use the approximate standard error of these latencies from Eq. (5) to give the statistic

$$(I_1 - I_2) / \sqrt{(\text{SE}[I_1] + \text{SE}[I_2])} \sim t_{\nu},$$

which will have the t distribution with ν degrees of freedom. A high or low value of this statistic is evidence

against the null hypothesis that the expected latencies are equal.

ACKNOWLEDGMENTS

This work was supported by the Wellcome Trust. M.D.R. is in receipt of a Wellcome Research Leave Fellowship.

REFERENCES

- DeYoe, E. A., Neitz, J., Bandettini, P. A., Wong, E. C., and Hyde, J. S. 1992. Time course of event-related MR: Signal enhancement in visual and motor cortex. *Proc. Soc. Mag. Res. Med.*, S1824.
- Boynton, G., Engel, S., Glover, G., and Heeger, B. 1996. Linear systems analysis of functional magnetic resonance imaging in human V1. *J. Neurosci.* **16**:4207–4221.
- Buckner, R., Bandettini, P., O'Craven, K., Savoy, R., Petersen, S., Raichle, M., and Rosen, B. 1996. Detection of transient and distributed cortical activation during averaged single trials of a cognitive task using functional magnetic resonance imaging. *Proc. Natl. Acad. Sci. USA* **93**:14878–14883.
- Friston, K. J., Jezzard, P., and Turner, R. 1994. Analysis of functional MRI time series. *Hum. Brain Mapping* **1**:153–171.
- Friston, K. J., Holmes, A. P., Poline, J.-B., Grasby, P. J., Williams, S. C. R., Frackowiak, R. S. J., and Turner, R. 1995a. Analysis of fMRI time-series revisited. *NeuroImage* **2**:45–53.
- Friston, K. J., Frith, C. D., Turner, R., and Frackowiak, R. S. J. 1995b. Characterising evoked hemodynamics with fMRI. *NeuroImage* **2**:157–165.
- Friston, K. J., Ashburner, J., Frith, C. D., Poline, J.-B., Heather, J. D., and Frackowiak, R. S. J. 1995c. Spatial registration and normalisation of images. *Hum. Brain Mapping* **2**:165–189.
- Friston, K. J., Williams, S., Howard, R., Frackowiak, R. S. J., and Turner, R. 1996. Movement related effects in fMRI time series. *Mag. Res. Med.* **35**:346–355.
- Friston, K. J., Josephs, O., Rees, G., and Turner, R. 1997. Nonlinear event-related responses in fMRI. *Mag. Res. Med.*, in press.
- Josephs, O., Turner, R., and Friston, K. J. 1997. Event-related fMRI. *Hum. Brain Mapping*, **5**:243–248.
- Rugg, M. D. 1995. ERP studies of human memory. In *Electrophysiology of Mind: Event-Related Potentials and Cognition* (M. D. Rugg and M. G. H. Coles, Eds.), pp. 132–170. Oxford Univ. Press, Oxford.
- Talairach, J., and Tournoux, P. 1988. *A Co-planar Stereotaxic Atlas of a Human Brain*. Thieme, Stuttgart.
- Thorpe, S., Fize, D., and Marlot, C. 1996. Speed of processing in the human visual system. *Nature* **381**:520–522.
- Vanderberghe, R., Josephs, O., Tyler, L. K., Price, C. J., Turner, R., and Friston, K. J. 1997. fMRI imaging of the spatiotemporal distribution of common and differential responses evoked by single sentences or random word sequences. *NeuroImage* **5**:S543.
- Worsley, K. J. 1994. Local maxima and the expected Euler characteristic of excursion sets of χ^2 , F and t fields. *Adv. Appl. Prob.* **26**:13–42.
- Worsley, K. J., and Friston, K. J. 1995. Analysis of fMRI time-series revisited—again. *NeuroImage* **2**:173–181.